Supplemental methods

a/LCI method

In the a/LCI setup (Fig. S1), low coherence light from a titanium:sapphire laser source (coherence length = 30 μm) is separated into input and reference beams, and a difference frequency of 10 MHz is introduced between the two via acousto-optical modulators. Exploiting the low coherence properties of the source, the retro reflector (RR) in Fig. S1 is translated along the optical axis to enable optical sectioning. Lenses L1-L4 are configured so that the incident light is collimated on the sample and lens L4 is in the conjugate plane of the scattered light (shaded in light blue in Fig. 2). L4 is scanned in the y-direction, and the intensity of the scattered light is obtained as a function of scattering angle. Both the reference and sample signals are focused on a balanced photodetector, generating a photocurrent which is demodulated at 10 MHz using a spectrum analyzer, yielding a signal proportional to the interference between the reference light and the scattered light from the sample RR and L4 are serially scanned so that a contour plot (Fig. S2) of the scattered light is built up as a function of sample depth and scattering angle.

The contour plot in Fig. S2, which depicts light scattered from a monolayer of MCF-7 cells, can be integrated over the region of interest to generate a plot of the intensity of the scattered light over angle, $S(\theta)$. The scattered light, $S(\theta)$ comprises a number of contributions. As is the case for all scatterers on the order of a wavelength or larger, there is a contribution from reflection/refraction, $R(\theta)$, and a contribution from diffraction $D(\theta)$, which arises due to the interference of light waves in the shadow of the scatterer. In the angular range observed in the present study, $R(\theta)$ is a slowly varying

component, non-oscillatory contribution to the scattering which includes scattering from organelles such as mitochondria, lysosomes, etc. as well as cytoskeletal proteins, which we denote $R_{sn}(\theta)$. $D(\theta)$ contains contributions to the scattering from: the cell nucleus, $D_{nuc}(\theta)$, higher-order correlations from nuclear scattering, subnuclear scattering, , and finally high-frequency noise.

Performing the Fourier transform on $S(\theta)$ yields the two-point correlation function of the optical field $\Gamma_S(r)$, which is associated with the two-point density correlation function of the sampled scatterers $\rho_S(r)$. Each spatial frequency corresponds to a different characteristic length scale within the sample given by the ratio of the wavelength and the subtended angle. Inspection of $\Gamma_S(r)$ guides a low pass filter to remove high frequency noise and the higher-order correlations, leaving $R(\theta)$, $D_{nuc}(\theta)$, and $R_{sn}(\theta)$. Most subnuclear scatterers are smaller than 2 μm in extent and thus for the angular range observed in the present study, this contribution will present as a slowly varying, non-oscillatory background in addition to $R(\theta)$. Therefore, by the removal of the best-fit 2^{nd} order polynomial, $D_{nuc}(\theta)$ is isolated.

The ILSA algorithm consists of a comparison of $D_{nuc}(\theta)$ to a database comprising a range of scattering distributions of spheroidal particles predicted by T matrix theory (discussed below). The most probable scattering configuration is deduced by performing a least-squares fitting algorithm between $D_{nuc}(\theta)$ and all elements of the database. The database is parameterized by equal volume diameter (EVD), aspect ratio (ε), the index of refraction of the medium n_b, the refractive index of the scatterer n_t, and the size distribution which is modeled as a normal distribution of sizes about the center EVD. The values for the present study are given in the main text. All scattering distributions in

the database consist of a diffraction component $D_{nuc,th}(\theta)$ and a reflection component $R_{th}(\theta)$, therefore a best-fit 2nd order polynomial is subtracted from all elements of the database to isolate $D_{nuc,th}(\theta)$ to compare only the contribution from nucleus diffraction.

The scoring system for the ILSA algorithm comprises two steps. The first is using a least-squares fitting algorithm across all parameters to establish the $D_{nuc,th}(\theta)$ with the lowest χ^2 value, χ^2_{min}. The second step is forming a list of all $D_{nuc,th}(\theta)$ with χ^2 values within 10% of χ^2_{min}. If any elements of this list have an EVD more than one half of a wavelength different than the best fit or an aspect ratio more than 0.03 different than the best fit, the best fit is considered degenerate and is discarded. If the best fit is discarded, the cutoff value for the low pass filter is reduced by one, and the fitting algorithm is run again. If the ILSA algorithm is still degenerate, the data point is not retained. This ILSA algorithm is well-established in the a/LCI literature[1, 2] using a Mie theory – based ILSA algorithm. The new element for the present study is extended the analysis to include aspect ratio in the algorithm.

The output of the ILSA algorithm is $D_{nuc,th}(\theta)$; the corresponding scattering distribution $G(\theta)$, which includes $R_{th}(\theta)$, is retrieved from the database. $G(\theta)$ is the predicted nuclear scattering from the ensemble of cellular scatterers. When $G(\theta)$ is subtracted from $F(\theta)$, the resulting distribution is $R_{sn}(\theta)$, the scattering distribution of subnuclear scatterers. The two-point density correlation function associated with this distribution, $\Gamma_{Dsn}(r)$, fits to a power law, indicative of self-similarity in the sample (over approximately 1-2 orders of magnitude). The exponent of the best-fit power law function, α, is associated with the fractal dimension, FD, as described in references[2]. The structure and organization of subnuclear scatterers is contained in the fractal

dimension measurement, therefore, FD can be a powerful indicator of changes in subcellular organization.

T-matrix based Light Scattering Database

The T-matrix method provides an efficient way to simulate scattering from spherical, spheroidal and other more complicated geometries. In order to simulate a large number of scatterers, a software program was developed that runs T-matrix simulations across numerous PCs, effectively reducing computation time by a factor of the number of processors available. This software is based on the extended precision (128 bit) public domain T-matrix code provided Mishchenko and was used to generate a light scattering database of spheroidal particles (3). We simulated equal volume diameters from 7.8 μm to 12.2 μm in increments of 40 nm, spheroidal aspect ratios from 0.56 to 0.90 (prolate) in increments of 0.01, background refractive indices of 1.35 and 1.36, scatter indices of 1.41 and 1.42, and an illumination wavelength of 830 nm. A normal size distribution with a 7% and a 10% standard deviation was used to model the typical variation in nuclear size. Each profile contained 48 scattering angles beginning with the backscatter angle and moving towards forward scattering in steps of 0.0103 radians. Each particle was simulated in 31 equally spaced orientations corresponding to rotating the cell nuclei about the plane of the glass substrate, and the orientations averaged to generate a composite orientation equivalent to a superposition of randomly orientated nuclei adhered to a glass slide.

To determine the range of refractive indices included in the database, QIA was used to guide an initial estimate for the EVD and ε, and a small database was prepared with refractive indices from 1.33 to 1.39 for the background refractive index and from 1.40 to 1.47 for the scattering refractive index. Fitting cell nuclei to the prepared database resulted in an average refractive in the range of 1.35 to 1.36 for the background refractive index and 1.42 and 1.43 for the scattering refractive index. There was no significant difference in refractive index between treated and untreated cells.

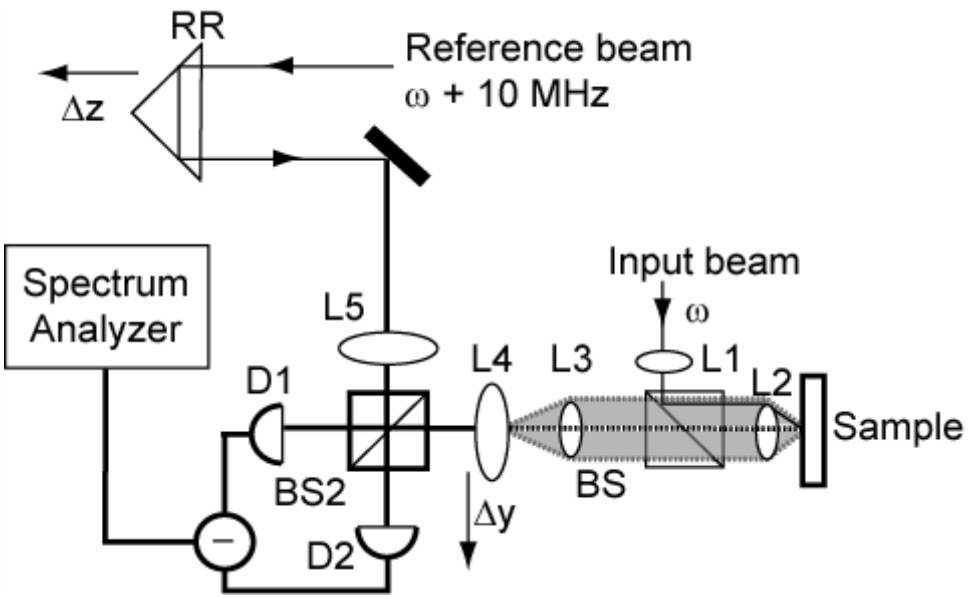

Fig. S1. Schematic of a/LCI setup.

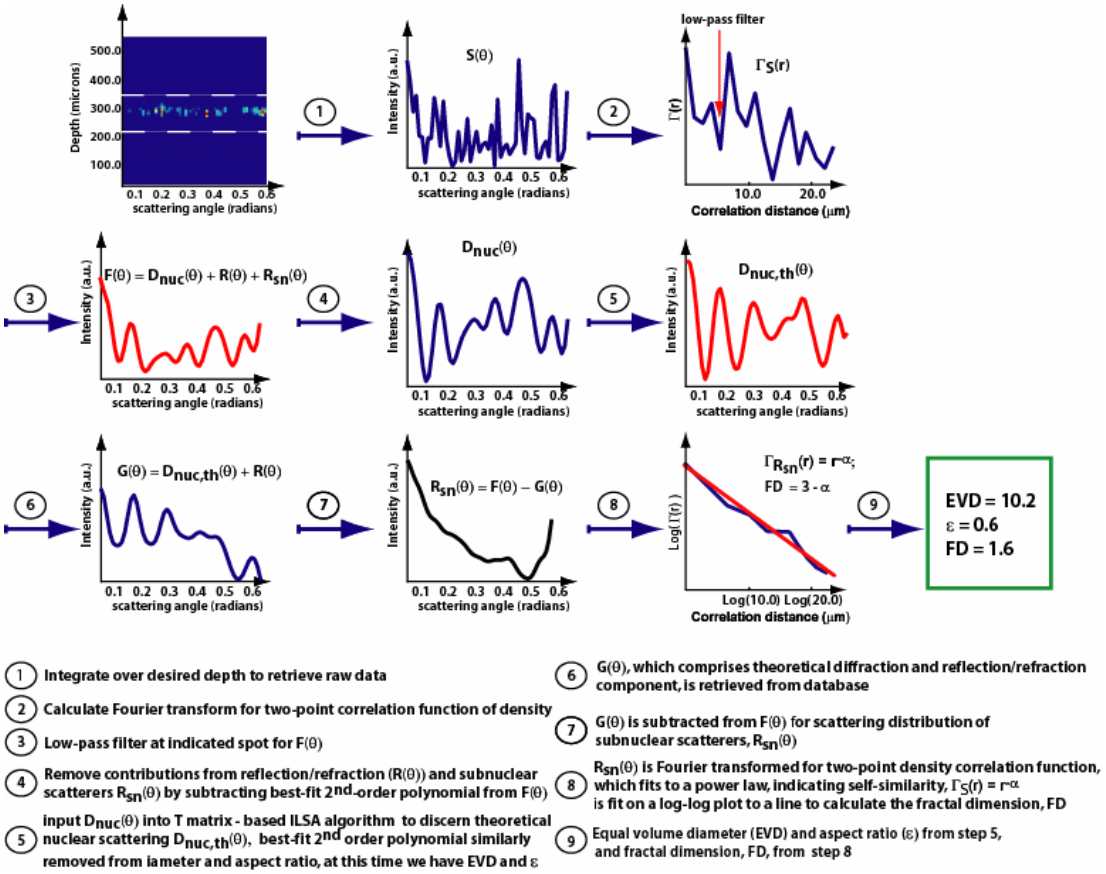

Fig. S2. Schematic of numerical processing involved in the a/LCI technique. Following the steps above using a T matrix based ILSA algorithm, the a/LCI technique can deduce the average equal volume diameter (EVD) and aspect ratio (ε) of the cell nuclei in a sample, as well as the fractal dimension (FD) of a biological sample.

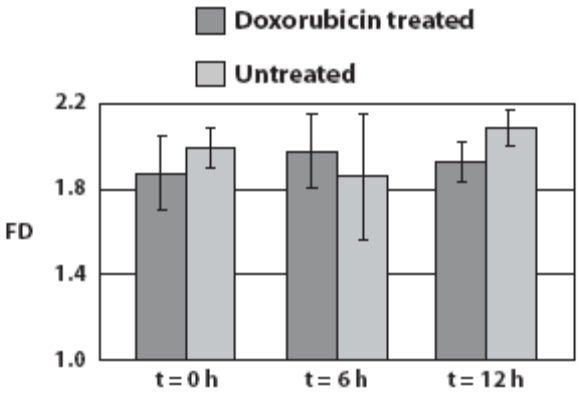

Fig. S3. Fractal dimension (FD) of MCF-7 cells treated with Doxorubicin. The FD was computed using a Mie theory – based ILSA algorithm, as opposed to a T matrix – based ILSA algorithm used in the text. No discernible pattern is present.

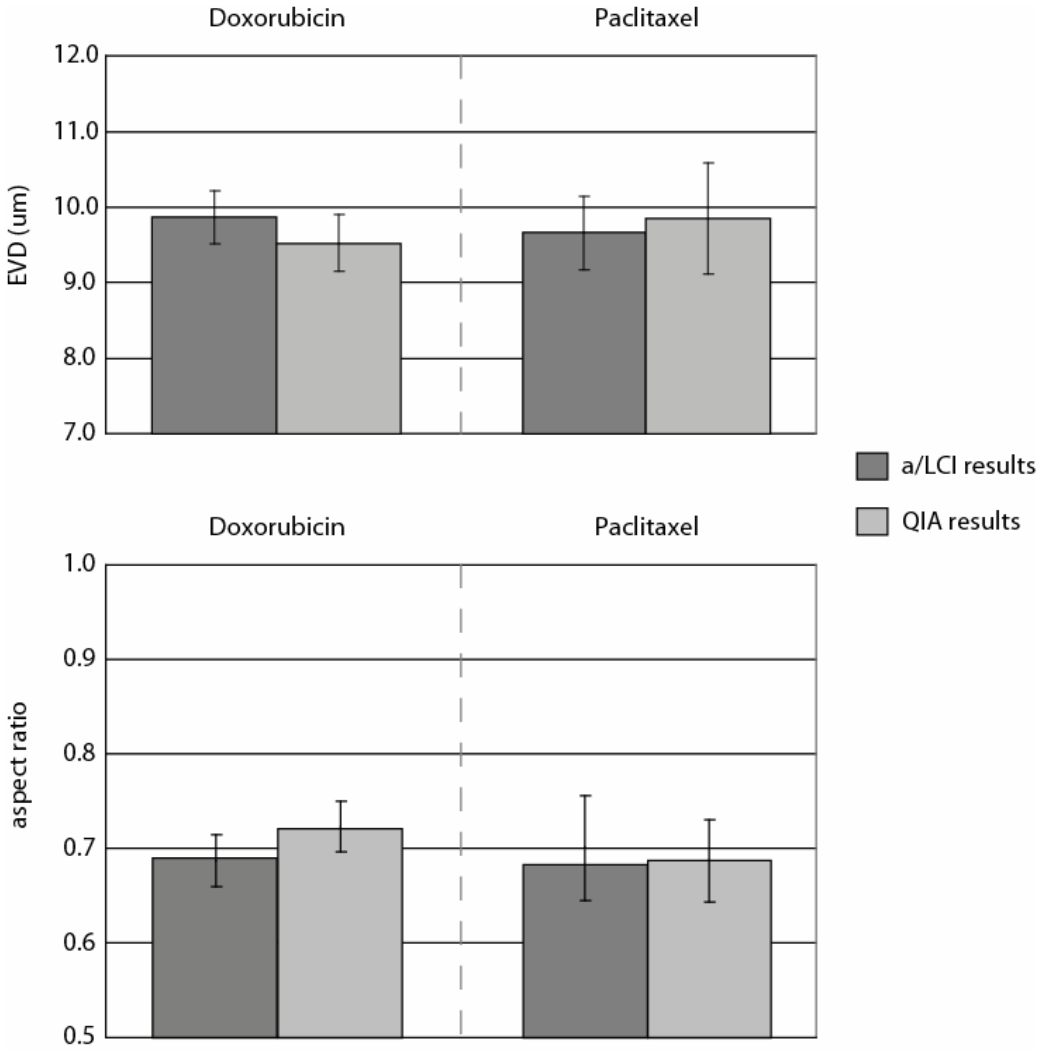

Fig. S4. Comparison of average EVD and aspect ratio of MCF-7 cell nucleus using a/LCI and QIA. Results based on three hour time point. A/LCI results were consistently very close to results of QIA at every time point. No morphological changes were seen during the observation window of 24 hours. a/LCI results based on 16 measurements while QIA based on 70 measurements.

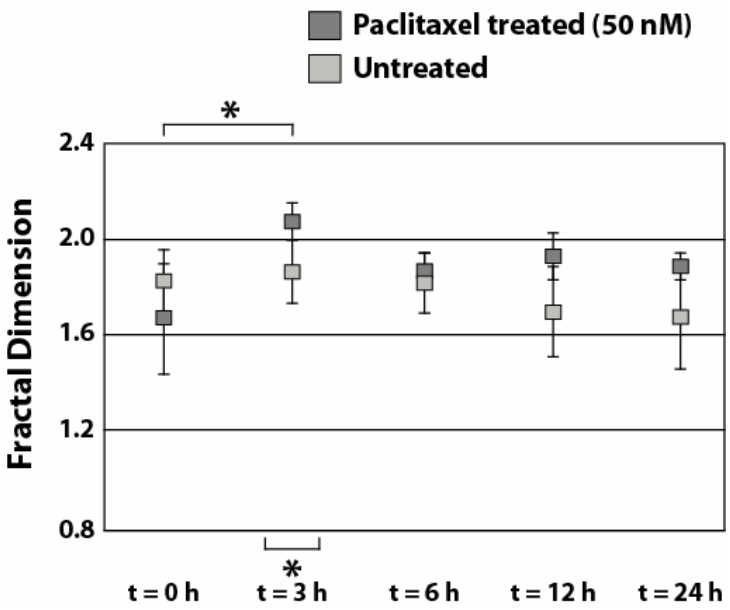

Fig. S5. Fractal dimension of MCF-7 cells treated with 50 nM Paclitaxel as assessed by a/LCI. Although early changes are seen, the fractal dimension appears to recover to approximately the same fractal dimension of untreated cells.

Supplemental References:

1. Pyhtila, J.W., R.N. Graf, and A. Wax, *Determining nuclear morphology using an improved angle-resolved low coherence interferometry system.* Optics Express, 2003. **11**(25): p. 3473-3484.
2. Wax, A., C.H. Yang, V. Backman, K. Badizadegan, C.W. Boone, R.R. Dasari, and M.S. Feld, *Cellular organization and substructure measured using angle-resolved low-coherence interferometry.* Biophysical Journal, 2002. **82**(4): p. 2256-2264.
3. Mishchenko MI, Travis LD, Hovenier JW. Light scattering by nonspherical particles : theory, measurements and applications. San Diego ; London: Academic; 2000